Observation of Cosmic Ray at the top of the Sierra Negra volcano in Mexico with the SciCRT prototype

E. Ortiz and J.F. Valdés-Galicia
Universidad Nacional Autónoma de México, Mexico City, 04510, México.

Y. Matsubara, Y. Nagai, and Y. Muraki
Solar-Terrestrial Environment Laboratory, Nagoya University, Furo-cho, Chikusa-ku, Nagoya 464-8601, Japan.

A. Hurtado, O. Musalem, R. García, and M.A. Anzorena
Universidad Nacional Autónoma de México, Mexico City, 04510, México.

L.X. González,
SCiESMEX, Instituto de Geofísica, Unidad Michoacán, Universidad Nacional Autónoma de México, 58190, Morelia, Michoacán. México.

Y. Itow, T. Sako, D. Lopez, and Y. Sasai
Solar-Terrestrial Environment Laboratory, Nagoya University, Furo-cho, Chikusa-ku, Nagoya 464-8601, Japan.

K. Munakata and C. Kato
Department of Physics, Shinshu University, Asahi, Matsumoto 390-8621, Japan.

S. Shibata, and H. Takamaru
College of Engineering, Chubu University, Kasugai 487-8501, Japan.

H. Kojima
Faculty of Engineering, Aichi Institute of Technology, Toyota 470-0392, Japan.

K. Watanabe
Institute of Space and Astronautical Science, Japan Aerospace Experiment Agency, Yoshinodai, Chuo-ku, Sagamihara 252-5210, Japan.

H. Tsuchiya
Japan Atomic Energy Agency, 2-4 Shirakata Shirane, Tokai-mura, Naka-gun, Ibaraki 319-1195, Japan.

T. Koi
SLAC National Accelerator Laboratory, Menlo Park, CA 94025-7015, USA.

Received 10 April 2015; accepted 25 September 2015

We are currently in the process of calibration of a new cosmic ray detector called SciBar Cosmic Ray Telescope (SciCRT) located at the top of the Sierra Negra volcano at 4,600 m.a.s.l., in Eastern Mexico. The SciCRT will work mainly as a Solar Neutron and Muon Telescope, with a high angular resolution ($\sim 1^{\circ}$), but it will also serve as a gamma ray and hadron shower detector. The mini-SciCR is a prototype of the SciCRT, it uses the same scintillator bars and recording hardware, the size of the mini-SciCR is 1/1568 compared with the SciCRT. In this paper we will report the main results obtained with the mini-SciCR that was operating at the top of the Sierra Negra volcano from October 2010 to July 2012. Our main aims were to show the appropriate performance of all the detector systems and to develop a tecnique to separate the flux of soft and hard secondary cosmic rays with the help of a Monte Carlo simulation, our energy range of interest is from 100 MeV to a few GeV. Aditionally we will report results with a modification of the detector setup that helped to confirm the correct identification of the particle species.

Keywords: Cosmic rays; secondary cosmic rays; SciCRT.

PACS: 95.55.Ev; 95.55.Vj; 95.30.Cq; 93.30.Hf

1. Introduction

When the primary cosmic radiation penetrates to the Earth's atmosphere, it is subject to interactions with the electrons, atoms and molecules that constitute the air. As a result of these interactions the particles suffer energy losses through hadronic and/or electromagnetic processes. Incident hadrons are subject to strong interactions when colliding with atmospheric nuclei, such as nitrogen and oxigen. Above an energy of a few GeV, local penetrating particle showers are produced, resulting in the creation of muons and other secondary particles in the collisions. Energetic primaries and, in case of heavy primaries, their spallation fragments continue to propagate in the atmosphere producing more particles along their trajectories in succesive interactions. The secondary cosmic radiation is divided into hard and soft components. The hard component is able to penetrate 15 cm of lead, which corresponds to 167 g/cm^2. The soft component which consists of positive and negative electrons and photons is almost completely absorbed in such a massive shield. Its flux at sea level amounts to about 35% – 40% of that of the muons [1].

The electron component in the atmosphere includes both primaries incident from outer space, and secondary that are created within the atmosphere. The main sources of secondary electrons of either charge are short-lived particles, resulting from interactions of primary and secondary cosmic rays with nuclei that constitute the air. Gamma rays from neutral pion decay undergoing pair creation supply the bulk of electrons and positrons, followed by decaying muons and, in rare cases, charged pions.

Muons are chiefly the decay products of charged pions and to a much lesser extent of charged kaons. With the exception of photons and neutrinos, muons are the most abundant component of the secondary cosmic radiation at sea level. Consequently much more information is available from muons than from any other component. In addition, muon data reveal information on high energy processes in the atmosphere and on the primary radiation, in particular on its spectrum and composition [2].

We are currently in the callibration process of a new type of detector called SciBar Cosmic Ray Telescope (SciCRT). The SciCRT will widen the capabilities of the current Solar Neutron Telescopes (SNT), that is, the ability to measure the energy and determine the direction of arrival of solar neutrons but with greater efficiency and precision, it will additionaly work as a Muon Telescope and be able to detect any kind of energetic particle crossing through and the showers that may produce inside [3].

In order to complete the callibration process we are currently operating in an intermitent manner just 3/8 of the full detector, therefore the importance of the particle discrimination has increased compared with that expected before the operation. The SciCRT is installed on the top of the Sierra Negra volcano, Mexico (575 g/cm^2; 18° 59′ N; 97° 18′ W). On this site we installed in October 2010 a prototype of this detector that uses the same scintillator bars that integrate the SciCRT and the same data acquisition hardware. This prototype was named mini-SciCR, the size of the mini-SciCR is 1/1568 of the volume of the SciCRT, our aims with this prototype detector were to diagnose the overall performance of the entire system on site, including the electronics, demonstrate that the mini-SciCR was able to detect particles of the secondary cosmic radiation and design some tecniques for the identification of the different species of arriving particles.

2. Mini-SciCR: detector prototype

The mini-SciCR (shown in Fig. 1) consists of 128 scintillator bars with a total volume of $20 \times 20 \times 20.8$ cm^3, arranged in eight layers, each layer consists of 16 bars integrating two mutually orthogonal planes of eight bars each. The scintillator bars are made of polystyrene, doped with PPO (1%) and POPOP (0.03%), to shift its emission spectrum peak to 420 nm. Each scintillator bar has dimensions of $2.5 \times 1.3 \times 20$ cm^3 with TiO_2 reflecting coating, it has a hole of 1.8 mm diameter in the middle, a wavelength shifting (WLS) fiber of 1.5 mm diameter is inserted for light collection, the gap between the fiber and the scintillator is negligible due to the low air density. The fiber is of the multi-clad type, Y11(200)MS, made by Kuraray, their absorption and emission spectrum has a peak in 430 nm and 476 nm respectively [4].

Each side of the detector (X and Y) has 64 scintillator bars whose emitted light is transported by WLS fibers attached to a 64 channel multi-anode photomultiplier tube (MAPMT) H8804 Hamamatsu Photonics K.K., its anodes are arranged in an 8×8 array with each anode measuring 2×2 mm^2. The sensitive wave length is from 300 nm to 650 nm, that matches the emission spectrum of the WLS fibers [5]. The photons emitted in every scintillator bar are collected and transported by WLS fibers to the MAPMT, the signals from it are read by an analog to digital converter (ADC). Once the ADC signal distributions have been determined and a proper discriminator established to discard the noise, the threshold signal level of each bar may be fixed (see below). For every event registered, the set of bars triggered establish the trajectory of the charged particles detected. To identify a neutron, a nuclear collision to produce a recoil proton is neccesary [5].

The readout system consists of two front end boards (FEBs) attached to each of the MAPMTs, a DAQ board connected to FEBs, and a trigger board (TB) connected to the DAQ board. The FEB is a combination of two ASICs (VA32_HDR11 and TA32CG) it is employed to mul-

tiplex pulse height information from each anode of a 64 channel MAPMT and make a fast triggering signal. The VA32_HDR11 has preamplifiers for 32 input channels and shapes its output with a slow Gaussian-like shaper, the TA32CG has discriminators to make a hit signal when a MAPMT anode signal exceeds the threshold level [6].

The DAQ board may readout eight MAPMTs, each of the eight channels has line drivers to control the FEB's ASICs and a flash ADC (FADC) to digitize the multiplexed analog signals. Programmable logic devices, CPLDs and an FPGA, are used to allow a flexible control of the data acquisition process. A CPLD (Xilinx XC95288), generates control signals for each FEB, it also provides a control sequence for digitization and storage of data into a FIFO. An FPGA (Xilinx XCV600) is connected to all CPLDs on the DAQ board to determine the timing to start readout and to switch data taking modes, it can also control timing to hold the peak of the shaped pulse using a fast triggering signal from each TA32CG [7]. The Trigger Board (TB) is connected to the DAQ board and makes the trigger signal, a hit signal is obtained when there is a signal from the upper 32 or the lower 32 MAPMT channels. The trigger signal is created by coincidence of the X side upper and the Y side upper hit signals, or/and X side lower and Y side lower hit signals. The cross-talk at the surface of a MAPMT was measured to be 2.72% for the central channels and 0.45% for the corners channels [7].

3. Performance of the mini-SciCR as a cosmic ray detector

The array of the scintillator bars of the mini-SciCR (see Fig. 1) served as the target and generator of tracks of the incident particles. To verify that the data of the detector are records of cosmic rays, we registered the counting rate of all particles that managed to cross the entire detector. It is difficult to make precise estimate of the mini-SciCR performance over the whole period of operation (October 2010 to July 2012) since some modifications to the original setup were performed extending for periods of up to four months (see below), in addition, there are periods where we have no data due to cuts in the power supply (see Fig. 2). It can be observed that data collection is stable when there was power to operate. In Fig. 2 we plot the hourly raw data obtained from October 2010 to March 2011, after which modifications to the original set up were made in periods of different lengths of time, we do not include periods in which modifications were made, since these changes were not consecutive, the data show fluctuations which may confuse the reader. Nonetheless, the Forbush decrease that occurred on March 7, 2012 was successfully registered by the mini-SciCR and gives us a tool to estimate its performance as a cosmic ray detector. In Fig. 3 we show a plot of the normalized counting rates of the mini-SciCR for the period 5 to 15 March, 2012, compared with those obtained by the neutron monitors (NMs) at [13] (1.1 GV cut-off rigidity), [8] (2.5 GV cut-off rigidity) and [6]

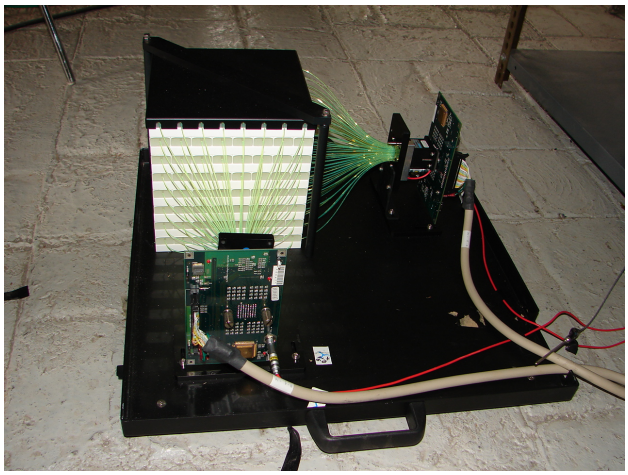

FIGURE 1. Photo of the mini-SciCR, showing one of the MAPMT and the FEBs.

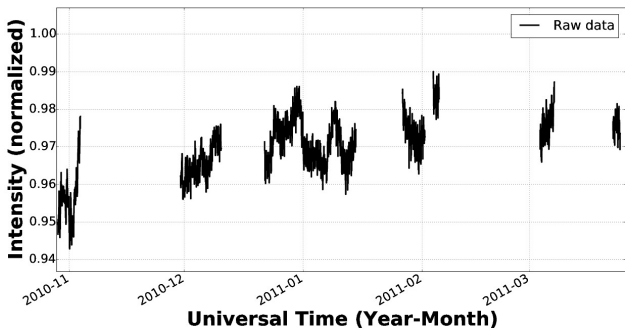

FIGURE 2. Hourly raw data of the mini-SciCR from October 2010 to March 2011 (vertical scale is normalized to 290,000 counts/hour), there are periods in which we have no data due to cuts in the power supply.

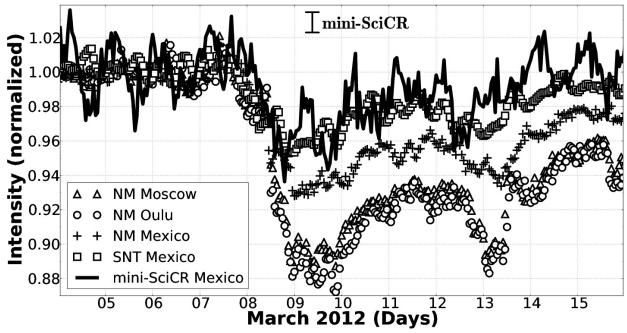

FIGURE 3. Forbush decrease on March 7, 2012, recorded by the mini-SciCR (line, normalized to 18,115 counts/hour), the >30 MeV charged particles channel of the Solar Neutron Telescope (square, normalized to 10,083,850 counts/hour) both installed in the Sierra Negra volcano summit, and the Neutron Monitors at Mexico City (plus sign, normalized to 812,210 counts/hour), Moscow (triangle, normalized to 550,260 counts/hour) and Oulu (circle, normalized to 379,200 counts/hour). The one sigma bar of the mini-SciCR is shown for reference. One sigma bars of other detectors would be unnoticeable.

(8.2 GV cut-off rigidity), plus the >30 MeV charged particles channel of the SNT at Sierra Negra [14]. The variability of the counting rates of the mini-SciCR is larger

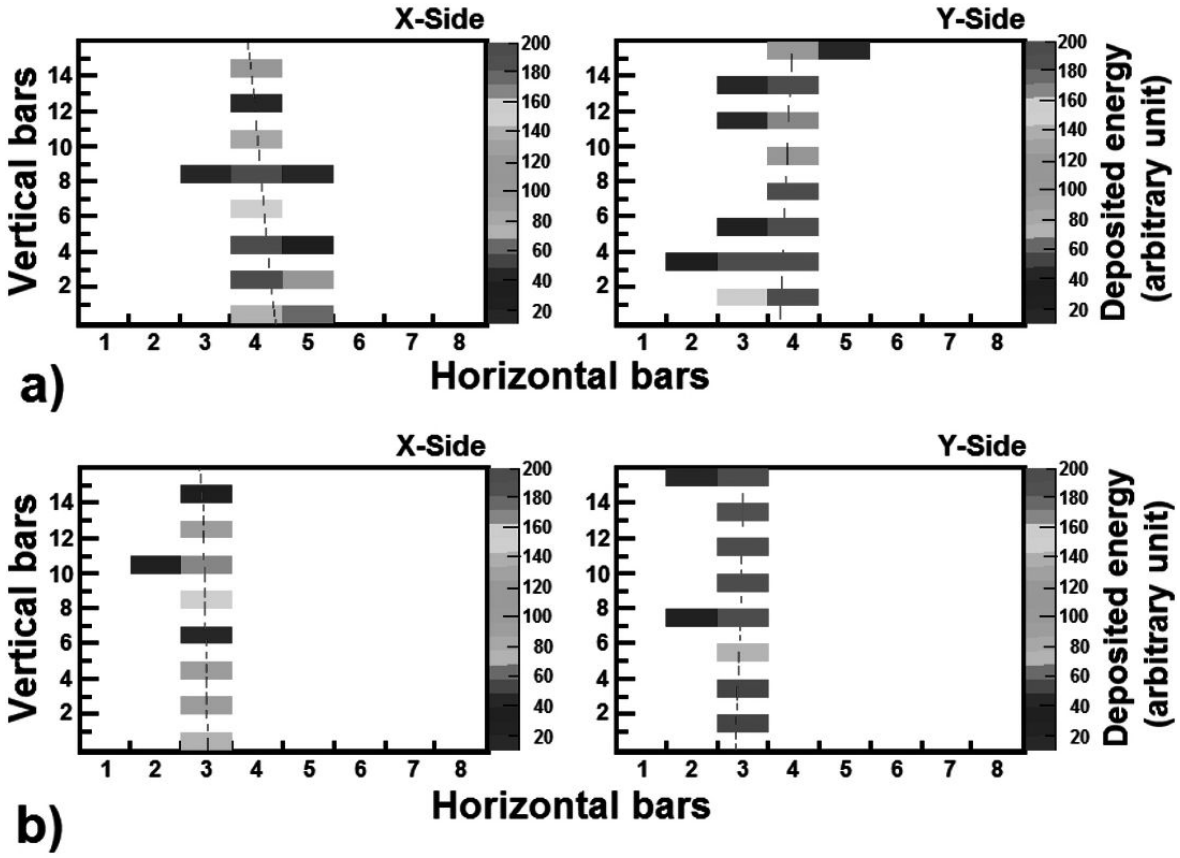

FIGURE 4. Traces left by a) an electron (400 MeV) and b) a muon (400 MeV), both are results of Monte Carlo simulations.

(288 counts/hour, see Fig. 3), as it should be expected regardless of the averaging period used, being a much smaller detector than the others with lower statistics. However, on the average, the amplitude of the Forbush decrease observed by mini-SciCR is remarkably similar to those of the SNT and its time evolution follows closely the decrease and recovery phase of the Mexico City NM. Oulu and Moscow NMs show deeper decreases as they respond to lower rigidity particles. Anyhow, it is to note the similarities observed in all detectors during the decrease and recovery phases. This result is a confirmation that the mini-SciCR detects cosmic radiation particles. A Forbush decrease is a global phenomenon of cosmic rays, to which all detectors around the world should respond in accordance with the rigidity cut-off of the site where it is located (see *e.g.* [1]). We are therefore confident that the counting rates of our prototype correspond to those of the secondary cosmic radiation.

4. Technique developed to separate the electron and muon fluxes

One of the main capabilities of the SciCRT will be the differentiation between species of particles leaving recognizable signals. At the atmospheric depth of Sierra Negra (575 g/cm^2), electrons and muons are by far the most abundant particles of the secondary cosmic radiation. As an additional performance test, it was therefore necessary to find a method to separate the muon and electron fluxes detected by the mini-SciCR.

We made a Monte Carlo simulation for the mini-SciCR, for this work, we consider electrons with kinetic energy between 100 MeV and 1 GeV and muons with kinetic energy between 100 MeV and 5 GeV, with zenith angles of incidence between 0° and 45° and flat momentum spectra for both species of particles. We used the PHITS package to calculate atmospheric attenuation and Geant4 to estimate particle behavior in the detector [10].

In search of criteria to differentiate between electron and muon signals left by their passage through the array of the scintillator bars, we made two different analysis of the results of a Monte Carlo simulation. First: we calculated the typical energy deposited by these particles as they pass through the scintillator bars, the results show that there is no statistically significant difference in the energy deposited by these particles. Second: we characterized the track left by these particles to pass through the array of the scintillator bars, the result of this analysis allowed us to establish a selection criteria to distinguish electrons from muons as will be described below.

In Fig. 4 we present examples of typical tracks left by an electron and a muon. It is easily recognized that the muon

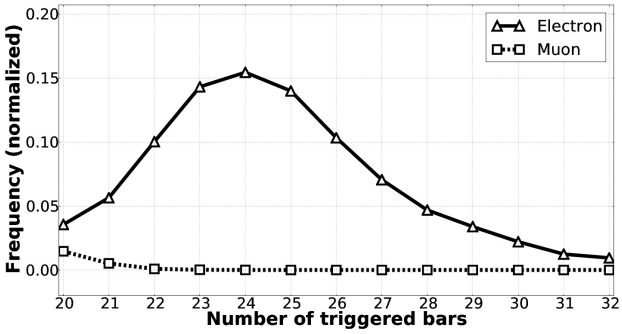

FIGURE 5. Distribution of number of triggered bars when electrons (triangle, normalized to 17,992 counts) or muons (square, normalized to 18,606 counts) pass through the mini-SciCR's array producing a small "shower" inside of the detector, because they triggered more than 19 bars (see text).

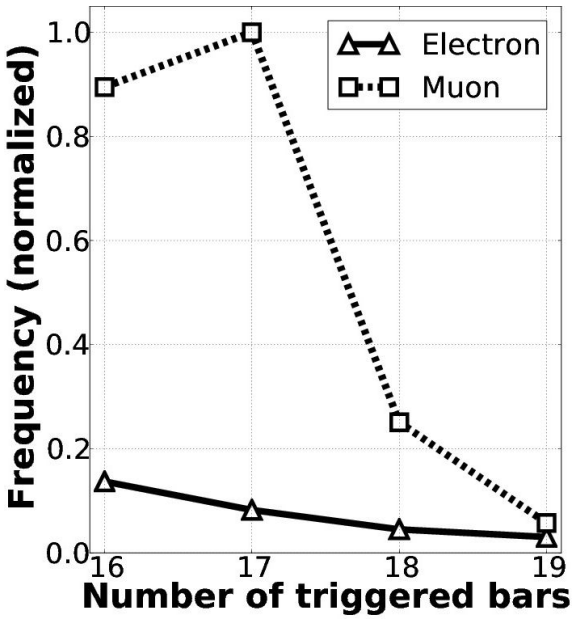

FIGURE 6. Distribution of number of triggered bars when electrons (triangle, normalized to 17,992 counts) or muons (square, normalized to 18,606 counts) pass through the mini-SciCR's array of the scintillator bars and they left "clean" tracks, because they triggered less than 20 bars (see text).

leaves a much "cleaner" track as it triggers almost only the bars through which the particle crosses (from 16 to 19), because the main energy loss processes are excitation and ionization [2]. In contrast, the electron trace is of the "shower" type (from 20 to 32 triggered bars), since electrons interact more easily with the matter they traverse as they add bremsstralung emission and Compton collisions to their energy loss processes ([4]). In both cases, in the energy range of interest. Therefore tracks with up to 19 bars triggered will be considered as "clean", alternatively those tracks triggering 20 or more bars will be labeled as "shower" type.

The analysis of tracks was made based on a Monte Carlo simulation of the mini-SciCR, consisted in counting the number of bars triggered when the electrons and the muons pass through the array of scintillator bars, with the condition that these particles cross all layers. To be able to cross the whole detector a particle must have a kinetic energy of at least 100 MeV. Our energy range of interest is from 100 MeV to a few GeV. We used these energy ranges since for them the fluxes of electrons and muons are dominant at the height of the Sierra Negra volcano summit (see, *e.g.*, [2,4]), 100 MeV is the lower limit of the Monte Carlo simulation program used. The main features of the results are summarized as follows:

1. When an electron crosses the array of scintillator bars, it may trigger from 20 to over 30 scintillator bars, the distribution obtained is independent of energy and shows a maximum around 24 (see Fig. 5). This indicates the generation of a small shower inside the array of scintillator bars, this happens because, besides the molecular excitation and ionization by the electrons, they also emit bremsstralung radiation, multiple Compton collisions are also plausible. However, there are few electrons that excite almost exclusively the bars along their path, generating "clean" tracks (see Fig. 6).

2. When a muon crosses the mini-SciCR, the number of triggered bars is generally less than those of the electrons. A muon excites almost exclusively the bars along its path, generating "clean" tracks, they essentially excite the molecules of scintillator material but do not emit bremsstralung radiation since this process is important for muons with energies greater than 200 GeV [2]. The distribution obtained shows a maximum at 17 bars, with a drastic drop towards higher numbers of bars (see Fig. 6).

3. The normalized distributions of the number of bars triggered, generated by electrons or muons that pass through the array of the scintillator bars of the mini-SciCR are very different: while muons show a sharp maximum at 17, the maximum of the electron distribution is at 24 bars, and it is much wider, due to the variety of processes by which electrons can deposit their energy in the scintillator material (this result is summarized in Table I). However, it should be noted that even with the strong capability to generate showers in the detector, the simulation shows that not all the electrons produce them, therefore there are some electrons that trigger less than 19 scintillator bars, independent of the electron energy.

Based on the simulation results, a suitable criteria for the separation of the fluxes of electrons and muons in the real tracks registred, needs to consider essentially the parts of the curves in Figs. 5 and 6 that do not overlap. An electron is considered a particle that leaves a track that triggered a number of scintillator bars greater than or equal to 20 and less than or equal to 32 (see Fig. 5), the electrons whose track is outside this range are 30% of those within the interval (see Fig. 6 and Table I). A muon is considered a particle that leaves a

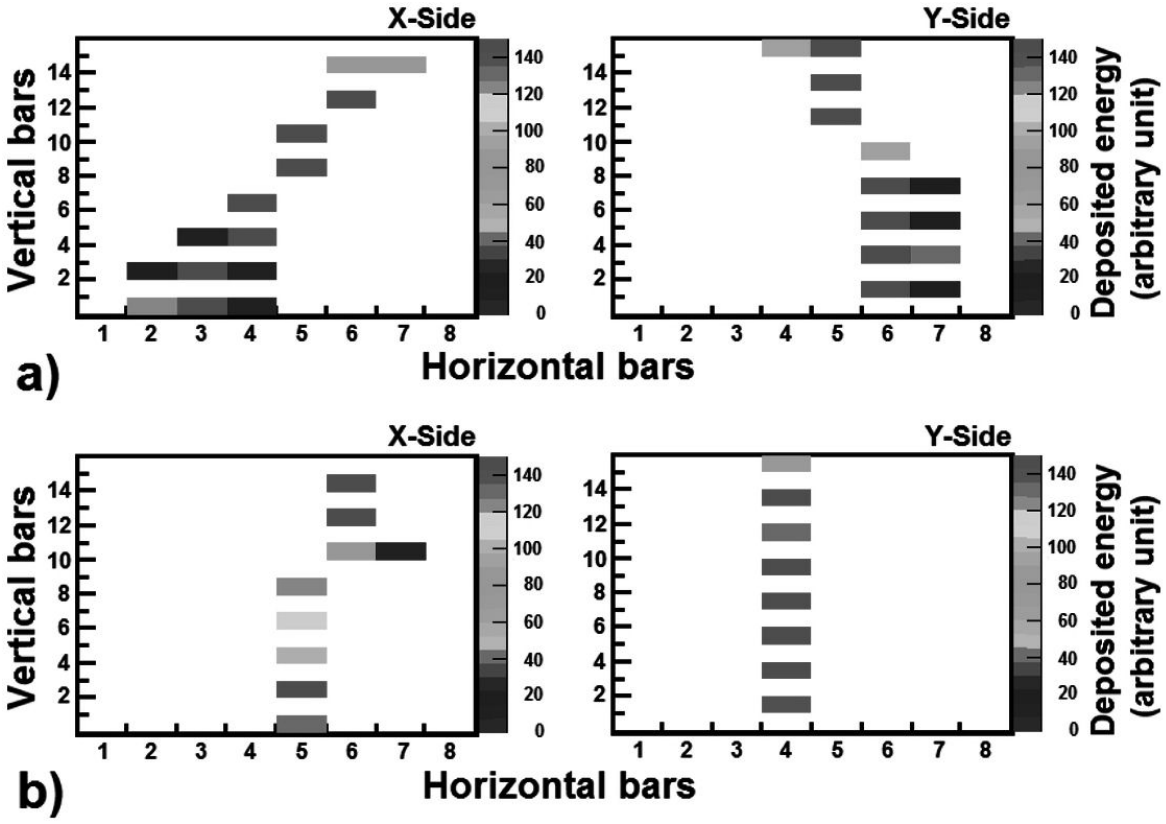

FIGURE 7. Traces obtained of the mini-SciCR data, considering the criteria for a) electrons and b) muons (see text).

TABLE I. Criteria for particle separation according to the number of triggered bars and overlap of the numerically obtained distributions.

Particle	Number of triggered bars	Maximum distribution	Overlap with other distribution
Muon	from 16 to 19 (clean track)	17	1%
Electron	from 20 to 32 (shower type)	24	30%

track that affects a number of scintillator bars greater than or equal to 16 and less than or equal to 19 (see Fig. 6), the muons whose track consists of a number of bars outside this range are slightly less than 1% of those within the interval (see Fig. 5 and Table I). In Fig. 7 we present examples of traces obtained with the mini-SciCR data.

With the above stated separation criteria, established based on the Monte Carlo simulations, we proceeded to analyse the tracks obtained in the mini-SciCR for the period from October 2010 to July 2012, when it was in operation at the Sierra Negra volcano. With the separation method designed, considering the overlapping of the simulation distributions (see Figs. 6 and 7), we made an estimate of the average flux of electrons that trigger from 20 to 32 bars as 4,400 $\pm$ 86 counts/hour. When we consider those tracks that are indistinguishable from muon tracks, the actual flux of electrons must be approximately 5,700 $\pm$ 122 counts/hour; the corresponding flux of muons estimated is of 14,000 $\pm$ 119 counts/hour, if we omit the calculated electrons that contribute to this counting rate because its track is indistinguishable to the muons, the actual flux of muons should be approximately 12,700 $\pm$ 130 counts/hour. These calculations were made for the flux observed inside the laboratory. These results are summarized in Table II.

TABLE II. Flux of secondary cosmic rays measured with mini-SciCR at the top of Sierra Negra Volcano.

Particle	Measured flux (counts/hour)	Flux corrected by overlap (counts/hour)
Muon	14,000 $\pm$ 119	12,700 $\pm$ 130
Electron	4,400 $\pm$ 86	5,700 $\pm$ 122

In order to confirm that the particles detected were indeed electrons and muons, we modified the original setup: it con-

TABLE III. Contribution of various sources to the total flux of electrons (5,700 $\pm$ 122 counts/hour) measured inside of the laboratory by the mini-SciCR.

Electron source according to the MC simulation	Contribution
Electrons of the secondary cosmic radiation	35.4%
Electrons produced by gamma rays	49.6%
Electrons produced by muons	15%

TABLE IV. Results of the experimental setup with lead plates.

Lead tickness (mm)	Experimental Muon flux (%)	MC simulation Muon flux (%)	Experimental Electron flux (%)	MC simulation Electron flux (%)
0	100.0	100.0	100.0	100.0
3.2	87.8	95.7	120.9	110.0
6.4	84.5	91.8	107.7	100.0
9.6	83.1	90.0	96.5	89.2
10	83.3	—-	100.5	—-
12.8	82.0	89.4	89.2	77.3
16	80.4	87.8	80.3	66.8
19.2	81.8	86.8	80.8	58.3
20	81.8	—-	73.6	—-
22.4	82.1	86.4	69.5	50.5
25.6	—-	86.1	—-	47.8
28.8	—-	85.7	—-	40.5
30	81.3	—-	64.1	—-
32.0	—-	84.2	—-	36.4
32.4	80.2	—-	66.0	—-
35	80.3	—-	60.0	—-
40	80.4	—-	61.4	—-
42.4	79.6	—-	65.2	—-
50	76.7	—-	47.4	—-

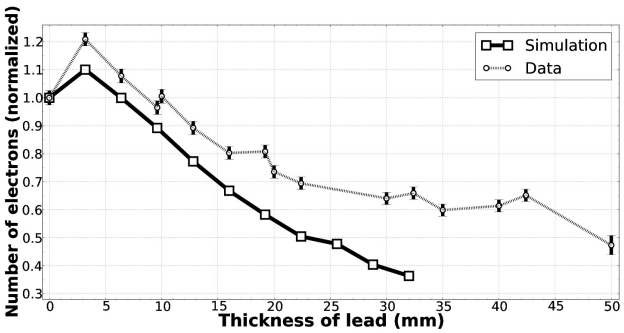

FIGURE 8. Electron flux as a funtion of the thickness of the lead plates over the mini-SciCR (normalized to 5,700 counts). The experimental data are the circles and the simulation data are the squares. The simulation results are the sum of all electrons originated by the three possible processes (see Fig. 10).

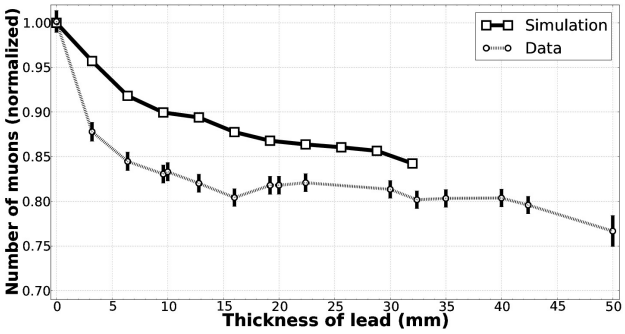

FIGURE 9. Muon flux as a funtion of the thickness of the lead plates over the mini-SciCR (normalized to 12,700 counts). The data of the experiment are the circles and the simulation data are the squares.

sisted on the emplacement of lead plates above the detector with varying thicknesses (from 3.2 mm to 50 mm). We also made a Monte Carlo simulation for these setups, including the roof and the wall of the laboratory (1 cm of iron).

As stated, the electron flux inside the laboratory is 5,700 $\pm$ 122 counts/hour, this quantity is the sum of: i) electrons of the secondary cosmic radiation that pass through the roof of the laboratory (35.4%), ii) electrons produced by gamma rays (pair production process) that interact with the material of the roof of the laboratory (49.6%) and, iii) electrons produced by muons (delta ray emission) that interact with the roof of the laboratory (15%). These contributions estimated by our Monte Carlo simulation are shown in Fig. 10 (ordinate scale for 0 mm of lead) and Table III. Taking the above considerations into account, the electron flux of secondary cosmic radiation inside of laboratory must be about 2,018 $\pm$ 139 counts/hour. We should also consider, however, the attenuation suffered by the electron flux in the roof, then the estimated flux outside the laboratory is $2,875 \pm 152$ counts/hour. Thus, the electron flux is about 23% of the muon flux at the top of the Sierra Negra volcano. These results are consistent with those obtained long ago in Mount Evans, Colorado at a similar height (4,359 m.a.s.l), where this ratio was 30% [7]. These fluxes coincide also with [4] and [2].

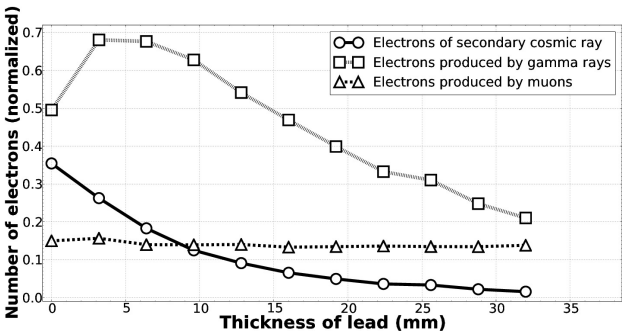

FIGURE 10. Numerical simulation results of the electron flux with different thicknesses of the lead plates over the mini-SciCR. The circles represents those produced in the atmosphere (secondary cosmic radiation), the squares are those comming from γ-rays that interact with the electrostatic field of the atoms of lead, and the triangles are those produced by muons.

Second, we included electrons with kinetic energy between 100 MeV and 1 GeV, γ-rays and muons with kinetic energy between 100 MeV and 5 GeV because they are the most abundant particles of the secondary cosmic radiation, all species with incident zenith angles between 0° and 45° and with an energy spectrum obtained from [2]. The results of this setup and the corresponding Monte Carlo simulations are shown in Figs. 8, 9, 10 and Table IV, and summarized as follows:

1. In the data with the first lead plate whose thickness is 3.2 mm, the number of electrons measured by the experiment increases by 20% over the average number of electrons measured without the lead plate; while the simulation data show an increase of 10% (see Fig. 8). The electron flux measured with the mini-SciCR covered with different thicknesses of lead is the sum of the electrons produced in the atmosphere (secondary cosmic radiation) that manage to cross the lead plates, plus those produced by γ-rays and muons that interact with the lead (see Fig. 10). One possible reason for the difference between the electron flux measured and that obtained in the simulation is that the γ-rays flux used in the simulation was obtained by interpolating data from [2] at different altitudes.

2. The results of the simulation (see Fig. 10) show that: 1) the number of electrons of the secondary cosmic radiation decreases with the increase in thickness of lead, 2) a production of electrons due to interaction of γ-rays with the lead (pair production), that is increased by placing the first lead plate, remains constant when placing the second plate and decreases for thicknesses of lead greater than 6.4 mm, 3) an almost constant production of electrons due to the interaction of muons with the lead (delta ray emission). The electrons produced by γ-rays are responsible for the increase in the electron counting rate observed when placing the first lead plate on top of the mini-SciCR. The sum of all the electrons originated by the three sources mentioned is shown in Fig. 8.

3. When the second lead plate (6.4 mm) is put on top of the detector, the number of electrons gradually decreases (see Fig. 8). After approximately 20 mm of lead, the flux becomes approximately constant for greater thicknesses of lead. The reason for this is these electrons are mainly produced by muons (delta ray emission), whose flux becomes approximately constant for these thicknesses of lead (see Fig. 9 and 10).

4. By placing 5 cm of lead (maximum thickness used) over the detector, the number of electrons decreased to 48.8% with respect to the original flux (see Fig. 8). The electron flux is not negligible since the muon flux is practically constant for thicknesses greater than 2 cm of lead, and these muons produce electrons by delta ray emission.

5. When lead plates are placed over the detector, the muon flux shows a decrease until about 1 cm thickness of lead (see Fig. 9). This indicates that the thickness is enough to stop a considerable ammount of muons, about 17% of the initial flux. Most probably these are slow muons and/or electrons that generate clean tracks (as explained above).

6. The muon flux has a less pronounced decrease for thicknesses of lead greater than 1 cm; it is almost constant, and with the maximum thickness of lead (5 cm) over the detector, it is 76.5% of the flux without lead plates over the detector (see Fig. 9), mainly due to the high energy muons that are able to cross all the lead plates.

7. In Fig. 8 the electron flux measured in the mini-SciCR is above the predictions of the simulation, in the simulation we used pure lead. In the experiment the lead used is not pure; the manufacturer guarantees a 90% pure lead composition of the plates, but we had no means to prove this is true; therefore the absorbing power of the plates used must be diminished with respect to pure lead.

8. In Fig. 9 we can see that the muon flux measured is below the simulation predictions. This is to be expected as the mini-SciCR is not able to detect all the high energy muons crossing through it. Differences are, however, never greater than 7%. Curves are almost paralell, with a slight tendency to converge at the highest thicknesses.

5. Summary

The capability of the mini-SciCR as a cosmic ray detector was demonstrated. As an example, we present the Forbush decrease recorded on March 7, 2012, that was also registered

by the charged particles channels of the SNT in Sierra Negra; Neutron Monitors of different cut-off rigidities, located around the world also detected the event with a similar structure as that observed at Sierra Negra. Therefore, we have shown that the technique to be used for cosmic ray detection in the SciCRT is reliable at the site.

Based on the number of scintillator bars triggered by particles crossing the detector, it was possible to establish a criterion to separate the records of electrons and muons. It was found that the electrons generally produce tracks with a greater number of bars triggered. These two species were chosen because they have a flux that is at least ten times more abundant than other secondary particles at the site where the detector was placed (575 g/cm^2). The criterion established does not produce a total separation of the two particle species, however it does provide tools to correct the observed counting rates.

Considering the previous paragraph, it was found that the flux of electrons inside the laboratory registered with the mini-SciCR is approximately 5,700 $\pm$ 122 counts/hour; after the proper corrections to consider the electrons produced at the roof of the laboratory are done (details in Sec. 4), the electron flux outside is 2,875 $\pm$ 152 counts/hours. The measured flux of muons should be approximately $12,700 \pm 130$ counts/hour. The ratio between the two fluxes at this atmospheric depth is consistent with those reported by Refs. 7, 4 and 2.

A modification of the original setup of the detector, putting lead plates of different thiknesses on top, combined with results of a MC simulation, lead us to verify that the fluxes separated by the technique designed consisted mainly of muons and electrons.

Acknowledgments

The authors sincerely thank the engineer Miguel Angel García Palacio for his technical support. This work was partially supported by PAPIIT-UNAM IN114612 and CONACyT-180727.

1. A.V. Belov, *International Astronomical Union* **257** (2009) 439-450.
2. P.K.F. Grieder, *ELSEVIER SCIENCE B.V.* (2001) 1-300.
3. M. Hasegawa, *Measurement of Neutrino Oscillation Parameters with Neutrino-Nucleus Interaction Studies in the K2K Experiment*, PhD thesis, Kyoto University, (2006) 24-38.
4. M.S. Longair, *High Energy Astrophysics*, Cambridge University Press, (1992) 1-151.
5. Y. Matsubara, *et al*., *Observation of solar neutrons by using a very sensitive cosmic ray detector*, 32nd International Cosmic Ray Conference, **10** (2011) 14-17.
6. *Mexico City Neutron Monitor*, http://cosmicrays.unam.mx/.
7. D.J.X. Montgomery, *Cosmic Ray Physics*, Princeton University Press, (1949) 186-283.
8. *Moscow Neutron Monitor*, http://cosrays.izmiran.ru/.
9. Y. Muraki, *et al*., *Astroparticle Physics* **29** (2008) 229-242.
10. Y. Nagai, *Performance of the SciCR as a solar neutron detector*, 32nd International Cosmic Ray Conference, **10** (2011) 2-5.
11. Y. Nagai, *et al*., *Astroparticle Physics* **59** (2014) 39-46.
12. K. Nitta, *et al*., *The K2K SciBar detector*, *Nuclear Instruments and Methods in Physics Research Section A* **535** (2004) 147-151.
13. *Oulu Neutron Monitor*, http://cosmicrays.oulu.fi/.
14. J.F. Valdes-Galicia, *et al*., *Nuclear Instruments and Methods in Physics Research Section A* **535** (2004) 656-664.
15. J.F. Valdés-Galicia, *Advances in Space Research* **43** (2009) 565-572.
16. M. Yoshida *et al*., *IEEE Transactions on Nuclear Science* **51** (2004) 3043-3046.